

AN ANALYSIS OF TURBULENT FLAME SPREADING  
IN A RECTANGULAR DUCT

Thesis by  
Richard E. Parks  
Lieutenant, United States Navy

In Partial Fulfillment of the Requirements  
For the Degree of  
Aeronautical Engineer

California Institute of Technology  
Pasadena, California

1963

## ACKNOWLEDGMENTS

I wish to express my appreciation for the guidance and helpful criticism of Professor Edward E. Zukoski, who originally suggested the problem. Thanks are also due to Professors W. D. Rannie and F. E. Marble for their interest and many helpful suggestions.

I also wish to thank Mrs. Roberta Duffy for the typing of the manuscript.

## ABSTRACT

The parametric equations for gas velocities and pressure, in terms of the density ratio and wake width, for a flame spreading in a rectangular duct from a point flameholder, are reviewed. A series solution for the cold gas velocity is proposed, evaluated, and its applicability to parametric values shown.

An attempt is made to determine the axial wake spreading rate, through a fluid mechanics approach utilizing the momentum equation and later the moment of the momentum equation. Both attempts are unsuccessful, for undetermined reasons.

The axial wake spreading rate is then approached, after defining an effective turbulent flame velocity, by equating the rate of disappearance of mass from cold stream with the rate of consumption of mass by the flame. Comparison is then made with a few of the conclusions that have been derived from experimental results.

## TABLE OF CONTENTS

<u>Part</u>	<u>Title</u>	<u>Page</u>
	Acknowledgments	
	Abstract	
	Table of Contents	
	List of Symbols	
I.	INTRODUCTION	1
II.	DEVELOPMENT AND DISCUSSION	3
	A. Parametric and Series Representations of Gas Velocity	3
	1. Development of General Equations	5
	2. Comparison with Experimental Results	7
	3. Series Representation	9
	B. Attempted Development of Axial Dependence	11
	C. Turbulent Flame Velocity Concept	15
	1. Comparison with Experimental Results	18
III.	CONCLUDING REMARKS	22
	References	24
	Tables	25
	Figures	27

# LIST OF SYMBOLS

$H$	distance from centerline to duct wall
$u_o$	initial approach velocity
$u_c(x)$	velocity in cold stream
$u_h(x)$	velocity in hot flame, occurring on centerline
$w$	distance from centerline to flame front
$x$	axial coordinate
$y$	vertical coordinate

$$\alpha(x) \quad u_c/u_o$$

$$\beta(x) \quad u_h/u_o$$

$$C \quad w/H$$

$$\eta \quad y/H$$

$$\lambda \quad \rho_h/\rho_c$$

$$\xi \quad x/H$$

$$\rho_c \quad \text{density in cold gas}$$

$$\rho_h \quad \text{density in hot gas}$$

$$\tau \quad \text{shear}$$

$$\gamma \quad v_t/u_o K\lambda$$

## I. INTRODUCTION

Laminar burning and the resultant wake spreading within channels have been analyzed, and the results compare well with experimental results. The success of the analysis may be attributed in part to an understanding of the phenomenon of laminar burning and the construction of an applicable analytic model.

Unfortunately, most technically interesting and practical flames are turbulent. The analysis of turbulent spreading rates has been significantly less successful than for laminar burning. The very complexity of the turbulent flame, involving changes in concentration due to diffusion and chemical reactions, coupled with turbulence makes an analytical model quite involved, and the solution even more forbidding. Analytical models for the turbulent flame front have been proposed, but applications of theories to flame propagation in ducts have not been possible. It has been experimentally observed that often the thickness of the flame front is small compared with duct dimensions. This has suggested theoretical treatments based on the assumption of a discontinuity in the gas density at the flame front. Results from this type of analysis by Scurlock<sup>(1)</sup> and later, and more simply, by Tsien<sup>(2)</sup>, have lead to parametric relations between wake width, gas velocities, pressure, and percent of fuel consumed. Spalding<sup>(3)</sup> more recently presented a theory of turbulent spreading based on a similarity between a spreading flame and a turbulent jet in which the dependence of spreading rate on axial distance is given.

Experimental work by Wright and Zukoski<sup>(4)</sup>, Satre<sup>(5)</sup>, and Thurston<sup>(6)</sup> has pointed up strong disagreement with Spalding's work

and with results obtained by extending the parametric relationships of Scurlock and Tsien with an assumption of a turbulent flame speed proportional to the laminar flame speed.

This paper is composed of three sections. The first section includes a slight extension of Tsien's work and the development of a series representation for gas velocity. A comparison is made of the series representation with values based on a theory similar to Dr. Tsien's which have been programmed on a digital computer. A comparison with experimental work is also included in this section. The second section had been suggested as a logical extension of the first by attempting to bring the spreading rate ( $x$  dependence) into the problem through the momentum equation. Unfortunately, the method was not successful, although several alternative approaches to the basic problem were attempted. The third section discusses a crude analysis of the problem based on the assumption that the turbulent flame speed depends upon the sum of the laminar flame speed and a turbulent term which is a function of density ratio and velocity gradient. The resultant spreading rates were compared to experimental values.

## II. DEVELOPMENT AND DISCUSSION

### A. Parametric and Series Representations of Gas Velocity

The physical model selected for this analysis is a gross simplification of the physical processes of the practical problem, as described in the introduction. In this model, we consider a steady, two-dimensional flow condition, with the flame front propagating from a point flameholder located on the centerline of a duct. The entering velocity profile is taken to be uniform and the flow, before and after the flame front, is assumed to be incompressible.

The flame front is approximated by a line discontinuity of density, temperature, and vertical velocity component, with a constant density on either side. In addition, no static pressure change occurs across the duct in a direction perpendicular to the axis of the flow.

In the interest of simplifying the calculations, the velocity profile is taken to be uniform in the unburnt flow, and is chosen to be linearly increasing from the unburnt value at the flame front to a maximum value at the duct centerline.

The flow discussed herein is depicted schematically in Figure 1. The assumption of incompressibility is valid for a low Mach number flow; that of constant static pressure is justifiable for a flame front at a small angle to the axis of the duct, as is the assumption of a continuous axial velocity at the flame front. The assumption of the velocity profile within the hot gas is open to question. Comparison with measured profiles, e. g. Ref. 7, show that, although the velocity profile in this region may have a good deal of detail, they can be reasonably represented by a linear profile, unless the detailed velocity gradients are important. In



this case, the simple linear velocity profile may lead to serious errors. The final assumption so far postulated is the representation of the flame front as a discontinuity. Detailed study of Schlieren photographs of turbulent flames<sup>(5, 6)</sup> show that the "flame" thickness may be as much as one centimeter. Further indication of this is given by examination of measurements of temperature and combustion efficiency within the flame. These likewise show a region, about a centimeter thick, of change rather than a thin discontinuity. Since duct widths of only fifteen centimeters are common in experiments, which are compared to the analytical results, it is evident that, although difficult to estimate, some degree of error must be induced by the discontinuity assumption.

Thus far, the problem as posed is exactly analogous to that discussed by Tsien<sup>(2)</sup>. As formulated, the problem can now be solved to give a parametric solution for flow velocities and pressures in terms of wake width with arbitrary density ratios. The solution is obtained through the utilization of three equations; Bernoulli's in the cold gas, and the equations of continuity and momentum integrated across the duct. These three equations involve five unknowns; cold gas speed, maximum burnt gas speed, pressure, wake width, and density ratio. Therefore, for arbitrarily selected values of density ratio, the first three variables may be given as a function of the wake width. In the following paragraphs, this process is shown briefly, and a simple representation in terms of a series expansion in the density ratio is given for the cold gas velocity. The resulting profiles are compared with experimental results.

(1) Development of General Equations. - The assumed velocity profile is given by

$$u = \begin{cases} u_c & y > w \\ u_h + \frac{y}{w} (u_c - u_h) & y < w \end{cases} \quad (1)$$

The equation of continuity may be written as an integral across the entire channel as

$$\int_0^H \rho u \, dy = \int_0^H \rho_c u_o \, dy .$$

Substituting the velocity profile and integrating as indicated gives for  $u_h$ :

$$u_h = \frac{2}{w\lambda} [H u_o - u_c (H-w)] - u_c . \quad (2)$$

The momentum equation in the axial direction is given by:

$$u \frac{\partial u}{\partial x} + v \frac{\partial u}{\partial y} = - \frac{1}{\rho} \frac{\partial p}{\partial x} + \frac{\partial}{\partial y} \left( \frac{\tau}{\rho} \right) . \quad (3)$$

Adding  $u$  times the differential form of the continuity equation to equation 3 and rearranging, one gets:

$$\frac{\partial(u^2)}{\partial x} + \frac{\partial(uv)}{\partial y} = - \frac{1}{\rho} \frac{\partial(\tau/\rho)}{\partial y} . \quad (4)$$

Writing this as an integral across the duct gives

$$\int_0^w \left[ \frac{\partial(\rho_h u^2)}{\partial x} + \frac{\partial(\rho_h uv)}{\partial y} \right] dy + \int_w^H \left[ \frac{\partial(\rho_c u^2)}{\partial x} + \frac{\partial(\rho_c uv)}{\partial y} \right] dy =$$

$$\int_0^w \left[ - \frac{\partial p}{\partial x} + \frac{\partial(\tau)}{\partial y} \right] dy + \int_w^H \left[ - \frac{\partial p}{\partial x} + \frac{\partial(\tau)}{\partial y} \right] dy . \quad (5)$$

From consideration of symmetry and physical arguments, the shear must be zero on the centerline, and since the velocity profile is considered to be uniform in the cold gas, the shear must be everywhere

zero in this region. Hence, shear at centerline and the duct wall is zero. Likewise, from symmetry, the vertical component of velocity is zero at the centerline and is also zero at the solid boundary of the channel wall. Hence, equation 5 may be written, after manipulation to put the differentials outside the integral, as

$$\begin{aligned} \frac{\partial}{\partial x} \int_0^w \rho_h u^2 dy - \rho_h u^2[w] \frac{dw}{dx} + \rho_h u[w] v_h[w] + \frac{\partial}{\partial x} \int_w^H \rho_c u^2 dy + \rho_c u^2[w] \frac{dw}{dx} \\ - \rho_c u[w] v_c[w] = \frac{\partial}{\partial x} \int_0^w -p dy + p[w] \frac{dw}{dx} + \frac{\partial}{\partial x} \int_w^H -p dy - p[w] \frac{dw}{dx}. \quad (6) \end{aligned}$$

The four terms outside of integrals on the left-hand side of equation 6 may be written as

$$\frac{u[w]}{dx} [-\rho_h u[w] dw + \rho_h v_h[w] dx + \rho_c u[w] dw - \rho_c v_c[w] dx] .$$

Here, the bracketed term is merely the mass flow in to and out of a differential area at the flame front, and hence the sum of these terms is zero. Then equation 6 becomes

$$\frac{\partial}{\partial x} \left[ \int_0^w (\rho_h u^2 + p) dy + \int_w^H (\rho_c u^2 + p) dy \right] = 0 .$$

Hence, the bracketed term in equation 6 is a constant along the axial direction, and may be evaluated in terms of its value at  $x = 0$ , as:

$$\int_0^H (\rho u^2 + p) dy = H(\rho_c u_o^2 + p_o) . \quad (7)$$

Bernoulli's equation in the cold stream may be written as

$$p_o = \frac{1}{2} \rho_c (u_c^2 - u_o^2) + p , \quad (8)$$

where the approximation is made that the component of axial velocity is so much greater than the vertical component that the magnitude of

the velocity is given by the magnitude of the axial velocity alone. For practical cases, this approximation will result in a negligible error.

Equations 2, 7, and 8 can be combined to eliminate  $v_h$  and  $p$ , and introduction of the dimensionless variables,

$$\lambda = \rho_h / \rho_c ,$$

$$\beta = u_h / u_o ,$$

$$\alpha = u_c / u_o ,$$

$$\eta = y/H ,$$

$$\zeta = w/H$$

gives the parametric solution for the velocity ratio,  $\alpha$ , in terms of the dimensionless wake width,  $\zeta$ .

$$\frac{4}{3\zeta\lambda} [1 - (1-\zeta)\alpha]^2 - \frac{2}{3} [1 - (1-\zeta)\alpha]\alpha + \frac{\lambda\zeta}{3} \alpha^2 + \alpha^2 \left(\frac{1}{2} - \zeta\right) = \frac{1}{2} \quad (9)$$

Solution for  $\beta$  is obtained from the continuity equation, equation 2; written in terms of the dimensionless parameters, the equation is:

$$\beta = \left\{ \frac{2}{\zeta\lambda} [1 - (1-\zeta)\alpha] - \alpha \right\}. \quad (10)$$

Numerical calculations for arbitrary values of the density ratio permit determination of dimensionless cold gas velocity,  $\alpha$ , and hence also dimensionless maximum hot velocity,  $\beta$ , and pressure distribution for all values of non-dimensional wake width. These results are shown in Table I and also in Figure 2.

(2) Comparison with Experimental Results. - In experimental work, a flameholder of finite size must be used to stabilize the flame in a duct; such flameholders are not treated within the framework of this analysis. However, the presence of this holder must be taken into consideration when comparing the results of theory and experiment.

The flameholder will have its attendant recirculation zone which may extend downstream a distance of five to ten flameholder diameters and, more significantly, may occupy up to thirty per cent of the duct height. Meaningful comparison between theory and experimental work, then, can only be made for experimental data beginning at the downstream end of the recirculation zone. In order to make such a comparison, an arbitrary beginning wake width must be specified for the theoretical case. In addition, it is noted that near the recirculation zone the velocity profile outside of the flame front is not flat, but has a slightly higher velocity near the flame front. This non-uniformity disappears further downstream, but must be taken into account, too.

Comparison is made in Figure 2 between theoretical and experimental values of cold gas speed as a function of wake width for three sizes of flameholders<sup>(4)</sup>. Both theory and results from the experiments are with a density ratio of about 0.16. The effect of the flameholder is seen as a significant deviation of the dimensionless cold gas velocity from theory near the centerline, but all curves approach that of theory at points far downstream of the influence of the flameholder and recirculation zone. This indicates that the analytical model chosen and assumptions made were reasonable, at least for the determination of gas velocities and pressures within the duct.

The comparison made here is typical of the agreement obtained between experiment and theory for turbulent flames. In a few isolated cases, complete velocity profiles have been obtained. Comparison is shown in Figure 3 of such a profile, from Reference 7, with the theoretical curve based on a value of wake width equal to 55 per cent of the

duct height. Despite the lack of symmetry of the experimental results, the curves agree reasonably in cold flow and in the hot flow near the edge of the flame. However, the centerline velocity error appears to be appreciable. This may be due in part to the fact that the centerline flow passed through the recirculation zone just downstream of the flameholder and thus may have a reduced total pressure.

In summary, it appears that the values of velocity and pressure estimated for a given wake width for the simple model proposed here do give a reasonable approximation of the flow field downstream of the flameholder and recirculation zone.

(3) Series Representation. - Unfortunately, the parametric results obtained from equation 10 are unwieldy to use in an attempt to obtain analytically the dependence of wake width, and hence other variables, on the axial distance from the point flameholder. Examination of equation 10 shows that it depends strongly upon the density ratio. In fact, as the density ratio goes to zero, i. e.,  $\lambda = 0$ , the equation has the particularly simple solution

$$\alpha = \frac{1}{1-\zeta}.$$

This result is merely a statement of the continuity equation in non-dimensional form, showing that for  $\lambda = 0$ , no mass is contained within the wake width. This suggests that a power series expansion in  $\lambda$  may lead to a convenient representation for the velocity in terms of the wake width. Because of the quadratic nature of 10, a series of the form

$$\alpha = \frac{1}{1-\zeta} [1 + f\lambda^{1/2} + g\lambda + h\lambda^{3/2} + \dots] \quad (11)$$

was proposed. The coefficients  $f$ ,  $g$ , and  $h$  were evaluated by

substitution of the series into equation 10, and then equating like powers of the density ratio,  $\lambda$ , within the resulting equation. The procedure is straightforward, but algebraically tedious; therefore, the details are omitted here. The results yield

$$f = -\sqrt{\frac{3}{8}} \frac{\zeta^{3/2}}{(1-\zeta)} .$$

$$g = -\frac{\zeta}{(1-\zeta)^2} \left( \frac{5}{8} - \zeta \right) ,$$

$$h = \sqrt{\frac{3}{8}} \left[ \zeta^{1/2} \frac{(-9 + 48\zeta - 27\zeta^2 - 30\zeta^3)}{48(1-\zeta)^3} \right] .$$

These coefficients can be evaluated for arbitrary values of  $\zeta$ , the normalized wake width, and are given in Table II for selected values. Note that once tabulated, calculation for dimensionless cold velocity, and hence other variables, for selected values of the density ratio is rapid. Moreover, the series gives a convenient analytical representation for the velocity as a function of  $\zeta$  and  $\lambda$ .

Convergence for the series for all values of wake width and density ratio is not guaranteed or implied. Comparison of values of  $\alpha$  computed from numerical solution of equation 10 with values obtained using the first four terms of the series is given in Figure 4 for a density ratio of 0.24. Close agreement is obtained out to  $\zeta = 0.6$  for this rather large density ratio: better agreement is obtained for smaller values of the density ratio. Since this range of density ratio and wake widths embraces the regions of practical interest, the series representation is a convenient and useful tool.

## B. Attempted Development of Axial Dependence

In this section, an outline is presented of an attempt to obtain the dependence of wake width, and hence other variables, on the axial distance from the point initiation of the flame. The approach used was to assume that the flame spreading process is governed primarily by turbulent mixing between hot burnt gas and cold combustible material. From this point of view, mixing processes are assumed to be slow in comparison with the chemical processes leading to combustion of the fuel-air mixture, and hence these mixing processes are the rate dominating step in the process. The latter point of view is suggested by the lack of dependence shown experimentally by the spreading rate on chemically dominated parameters such as the laminar flame speed.

Application of the assumption is made by carrying out integrals of the momentum equation in a manner such that the axial coordinate appears explicitly in the result. In order to do this analytically, the series representation derived in the previous section is used to eliminate gas velocities and leave the momentum equation in terms of a differential equation involving the axial coordinate and wake width.

To carry out this procedure, the shear term must be given explicitly. This is accomplished through use of the mixing length hypothesis first formulated by Prandtl in 1925, and is based to a great extent upon physical reasoning. Basically, it is argued that the average value of the random fluctuations of axial velocity,  $u'$ , is proportional to a characteristic length times the change in the mean value of axial velocity in the vertical direction, i. e.,  $u' \sim l \frac{du}{dy}$ . Further, the assumption is made that the average value of the random fluctuations in



the vertical direction,  $v'$ , is proportional to the same quantity,

$v' \sim \ell \frac{du}{dy}$ . Then the expression for the Reynolds stress becomes

$\tau \sim \rho \ell^2 \frac{du}{dy} \left| \frac{du}{dy} \right|$ . In our case, the choice of velocity profile gives

$\left| \frac{du}{dy} \right| = (u_h - u_c)/w$ , and further, the only characteristic or mixing dimension within the problem is the wake width,  $w$ ; hence, the form for shear in our analysis becomes:

$$\tau = k \rho_h w (u_h - u_c) \frac{du}{dy} \quad (12)$$

where  $k$  is an undetermined proportionality constant. This particular form for the shear has been chosen to give  $\tau = 0$  outside of the flame zone and is consistent with the assumed velocity profile.

Consider again the momentum equation coupled with the equation of continuity given in the first section,

$$\frac{\partial}{\partial x} (\rho u^2) + \frac{\partial}{\partial y} (\rho uv) = - \frac{\partial p}{\partial x} + \frac{\partial}{\partial y} (\tau) \quad .$$

In order to keep the  $x$  dependence in the equation, it is necessary to integrate this equation over only a part of the wake width. Here, it is chosen to integrate from the centerline to one-half the wake width.

Carrying out this integral and utilizing the Bernoulli assumption in cold gas for pressure dependence, one gets

$$\int_0^{w/2} \frac{\partial}{\partial x} (\rho u^2) dy + \rho u \{w/2\} v \{w/2\} + \int_0^{w/2} - \rho_c \frac{\partial (u_c^2/2)}{\partial x} dy = \tau \{w/2\} \quad ,$$

where equation 12 can be used to express values of  $\tau$ . The vertical velocity component,  $v$ , is eliminated by use of an integral of the continuity equation, as

$$v \{w/2\} = - \int_0^{w/2} \frac{\partial u}{\partial x} dy \quad .$$

Manipulation of these equations in order to get all differentiation outside of the integrals results in

$$\frac{\partial}{\partial x} \int_0^{w/2} u^2 dy - u[w/2] \frac{\partial}{\partial x} \int_0^{w/2} u dy - \frac{\rho_c}{\rho_h} \frac{w}{2} \frac{\partial \left( \frac{u_c^2}{2} \right)}{\partial x} = \frac{\tau[w/2]}{\rho_h}.$$

Evaluating the shear,  $\tau$ , as suggested above, substituting for  $u[y]$ , and rewriting in non-dimensional form gives, finally:

$$\begin{aligned} & \frac{\partial}{\partial \xi} \left[ \frac{\zeta}{24} \left( \alpha^2 \left\{ \frac{28}{\zeta^2} (1-\zeta)^2 + \frac{20\lambda}{\zeta} (1-\zeta) + 4\lambda^2 \right\} + \alpha \left\{ \frac{-56(1-\zeta)}{\zeta^2} - \frac{20\lambda}{\zeta} \right\} + \frac{28}{\zeta^2} \right) \right] \\ & - \frac{1}{\zeta} \left[ 1 - (1-\zeta)\alpha \right] \frac{\partial}{\partial \xi} \left[ \frac{\zeta}{8} \left( \alpha \left\{ \frac{-6(1-\zeta)}{\zeta} - 2\lambda \right\} + \frac{6}{\zeta} \right) \right] - \frac{\lambda\zeta}{2} \frac{\partial \left( \frac{\alpha^2}{\zeta^2} \right)}{\partial \xi} \\ & = -k \left[ \frac{4}{\zeta^2} \{ 1 - (1-\zeta)\alpha \}^2 - \frac{8\lambda\alpha}{\zeta} \{ 1 - (1-\zeta)\alpha \} + 4\lambda^2 \alpha^2 \right]. \end{aligned} \quad (13)$$

This equation involves the dimensionless variables, wake width  $\zeta$ , axial distance  $\xi$ , and cold velocity  $\alpha$ . Thus, solution of this equation will give a value for rate of flame spreading in the axial direction, providing only that  $da/d\zeta$  and  $\alpha$  may be obtained as functions of  $\zeta$ . This requires either the use of the series representation for  $\alpha$ , equation 11, or a numerical solution utilizing computed tables of gas velocity versus wake width obtained from equation 10.

To obtain an analytical solution, the series solution for  $\alpha$  was substituted in equation 13. The resultant differential equation was then separated into a number of separate equations by equating coefficients of equal powers of the density ratio,  $\lambda$ . Again, the process is essentially straightforward but extremely tedious, and details are omitted here.

The results were that equations of the coefficients of the zero<sup>th</sup>,

one-half, and first powers of the density ratio were identically satisfied. The first non-trivial relation occurred in coefficients for the cube of  $\lambda$  and is given, after reduction, by

$$\left[ -\frac{29}{96} - \frac{19}{48} \frac{\zeta}{1-\zeta} + \frac{1}{3(1-\zeta)} \right] \frac{d\zeta}{d\xi} = k.$$

Examination of the bracketed term indicates that a change occurs when  $\zeta = 1/3$ . This result is physically unrealistic. The second non-trivial relation exhibits a like behavior.

It was first thought that this behavior might be a result of the use of the series expansion for  $\alpha$ . To test the validity of the use of the series representation in the solution, a numerical solution of equation 13 was performed using parametric values of gas velocity and wake width given in Table I. This calculation also exhibited a change in sign of  $d\zeta/d\xi$  in the vicinity of one-third the wake width. Although effectively removing the series representation from the doubt of credulity, this does not provide any insight into the reason for the apparent failure of what appears to be a plausible approach.

In an attempt to vary the approach slightly, the moment of the momentum equation was used in lieu of the momentum equation as a starting point for the calculation. That is,

$$u \frac{\partial(u^2/2)}{\partial x} + v \frac{\partial(u^2/2)}{\partial y} = -\frac{u}{\rho} \frac{\partial p}{\partial x} + u \frac{\partial}{\partial y} \left( \frac{\tau}{\rho} \right) \quad (14)$$

was used.

Manipulation of this equation along the same lines as suggested in the previous calculation and then integrating from the centerline to the edge of the wake yields

$$\frac{\partial}{\partial x} \int_0^w u \left[ \frac{u^2}{2} - \frac{u_c^2}{2} \right] dy + \left( 1 - \frac{\rho_c}{\rho_h} \right) u_c \frac{\partial u_c}{\partial x} \int_0^w u dy = -k (u_h - u_c)^3.$$

Evaluating the integrals, rewriting in dimensionless form, and manipulation yields:

$$\begin{aligned} \frac{\partial}{\partial \xi} \left[ c \left[ \left( \frac{1 - \alpha(1-c)}{c\lambda} \right)^3 - \alpha \left( \frac{1 - \alpha(1-c)}{c\lambda} \right)^2 \right] \right] + \left( 1 - \frac{1}{\lambda} \right) \alpha \frac{d\alpha}{d\xi} \frac{1}{\lambda} [1 - (1-c)\alpha] \\ = -k \frac{8}{c^3 \lambda^3} [1 - \alpha(1 - c + c\lambda)]^3. \end{aligned} \quad (15)$$

Again, making the series substitution for  $\alpha$ , then multiplying through by  $\lambda^3$  for convenience, and equating like powers of  $\lambda$ , it is found that the first non-trivial expression is

$$\left[ -\frac{5}{16} - \frac{3c}{8(1-c)} + \frac{1}{3(1-c)} \right] = k,$$

which is almost identical to that obtained previously from the momentum equation, and which also exhibits the peculiarity of  $dc/d\xi$  changing sign at a wake width of one third. The equation from the next higher power of  $\lambda$  also shows this behavior.

No satisfactory explanation has been found as yet for this unrealistic behavior of the solutions. However, it may be due to specifying a straight-line velocity profile, or any velocity profile satisfying a similarity relation of the type used in the parametric analysis of the first section. This, and the infinitely thin flame front, are the most dubious assumptions made within the analysis. Validity of the other assumptions might be questioned in a quantitative sense, but should not impair the behavior of the solution.

### C. Turbulent Flame Velocity Concept

Previous analyses have assumed the turbulent flame speed to

be simply proportional to the laminar flame speed. These theories do not agree well with experimental results obtained with turbulent flames.

In this section, we shall use an approach analogous to the turbulent mixing hypothesis. The average turbulent fluctuation in vertical velocity  $v'$  has been described by Prandtl and von Karman, from purely physical reasoning, as proportional to a characteristic length times the rate of change of axial velocity in the vertical direction. Actually, the argument is made for the average turbulent fluctuation in the axial direction,  $u'$ , and then it is assumed that  $u'$  and  $v'$  are of the same order. In our specific example, the rate of change in axial velocity in the burnt gas is merely  $(u_h - u_c)/w$ , and since  $w$  is also the characteristic length, the average turbulent fluctuation in the hot gas is proportional to  $u_h - u_c$ . From our earlier analysis it was shown that the vertical components of velocity were discontinuous at the flame front and were inversely proportional to the density ratio across the flame front. Hence the fluctuating vertical component of velocity on the cold side is proportional to  $\lambda(u_h - u_c)$ . Then the mass consumption rate would be given merely by  $\rho_c \lambda K(u_h - u_c)$ , where  $K$  is an unspecified proportionality constant.

Hence, the mass consumption rate is given by  $\rho_c \lambda K(u_h - u_c)$ , where  $\lambda K(u_h - u_c)$  may be construed as a flame velocity. The overall flame velocity would also seem to require a consideration of the laminar flame velocity as well. In fact, if the laminar component is not considered, the turbulent component would lead to a flow which could never be started, since at the origin the velocity differences do not exist. Accordingly, an effective turbulent gas velocity was defined as

$$v_f = v_l + K\lambda(u_h - u_c) . \quad (16)$$

The axial coordinate can now be introduced in a natural manner by equating the rate of disappearance of mass from the cold gas stream to the rate at which the flame front advances times the density. This mass balance is given by

$$\frac{d}{dx} [\rho_c u_c (H-w)] = - \rho_c K\lambda \left[ \frac{v_l}{K\lambda} + u_h - u_c \right] , \quad (17)$$

providing the angle between the flame front and the axial direction is small. In general, this approximation is a valid one for practical problems.

Equation 17 may be rewritten in dimensionless form as

$$\frac{d}{d\xi} [\alpha(1-\zeta)] = - K\lambda [\gamma + \beta - \alpha] , \quad (18)$$

where  $\gamma = v_l / (K\lambda u_o)$ .

For numerical computations utilizing Table I, this equation becomes:

$$\frac{\Delta[\alpha(1-\zeta)]}{(\gamma + \beta - \alpha)} = - K\lambda \Delta\xi . \quad (19)$$

Using this form, axial coordinates were calculated from Table I for  $\lambda = 0.16$  with arbitrary values of  $\gamma$  varying from nearly 0 to 0.2. The results are presented in Figure 5. Due to the form of the equation, the calculation breaks down near the origin for values of  $\gamma$  approaching zero, and the development from the point source will never occur. To avoid this difficulty in presentation, the results are also given in Figure 6, where the common origin has been chosen as the point where the flame front touches the channel wall. This removes the arbitrariness in starting for values of  $\gamma$  approaching zero. Note that the profile for all the curves is very nearly linear in that portion of the duct from about

0.2 to 0.8 of the duct height, and are not very sensitive functions of  $\gamma$ .

(1) Comparison with Experimental Results. - A typical flameholder and its attendant recirculation zone may influence the flow for from five to ten flameholder diameters downstream, and the wake width at the end of the recirculation zone may be as much as 30 per cent of the duct height. The velocity profile at the end of the recirculation zone is not that postulated for the hot gas, but has been found to approach this within a short distance. Thus, the flame studied experimentally usually starts off with an appreciable width and with a velocity profile different from that postulated in this analysis.

Since the flame holding region is fixed primarily by geometric considerations<sup>(4, 5, 6)</sup>, the starting width will not change appreciably with either gas temperature, fuel-air ratio, or approach stream speed. Thus, in comparing theoretical with experimental results, it is appropriate to consider theoretical curves with arbitrary values of original wake width at the axial origin of the problem. This is shown in Figures 7 and 8 for density ratios of 0.16 and 0.24 and with starting wake widths of 0.1 and 0.3 of the duct height.

The selection of arbitrary values of  $\gamma$  varying from 0 to 0.2, to be presented as typical, was predicated upon the fact that the laminar flame speed was small in comparison with initial flow conditions. To justify this assumption, it is necessary to evaluate the proportionality constant, generated by the mixing length concept of Prandtl. This can not be done from a theoretical point of view. Hence, an estimate for the approximate magnitude of  $K$  is sought by a comparison of experimental and theoretical results. Comparison between Figure 8, Ref. 4 and

Figure 8 gives a value for  $K$  approximately equal to one third.

Typical values for laminar flame speed, approach speed, and density ratio give values for  $\gamma$  which are in the range 0 to 0.2.

Two of the conclusions reached by Wright and Zukoski<sup>(4)</sup>, which summarize as well the results of Refs. 5, 6, and 7, were that: (1) the flame spreading rate is independent of approach flow speed, and (2) that the density ratio is not very important in fixing the flame spreading rate. It is now desired to compare the results of this analysis with conclusions reached from experimental work. Within this analysis, the only effect of changing the approach speed would be to change the value of the parameter  $\gamma$ . A doubling of the approach speed would result in  $\gamma$  being reduced by a factor of one half. Comparing values of flame spreading rate (slope of the curve) for values of  $\gamma = 0.2$  and  $\gamma = 0.1$ , it is noted that there is, at most, a change of a percent or two. A comparison of actual wake width as a function of an arbitrary axial distance from Figure 7 indicates a variation of six or seven per cent, when an initial wake width of ten per cent is used. For the 30 per cent initial wake width, the variation is less. Thus, the theoretical dependence of spreading rate on velocity agrees well with the experiments; the actual wake width variation is somewhat larger for the theory. This may be partly attributed to the artificiality of the starting condition, since it would be expected that slope and distance would be nearly matched in starting in both cases. The slight variation in spreading rate is felt to be more significant, since the slope condition is inherently the more demanding problem. This extremely small variation is felt to be consistent with experimental conclusions, since such a slight effect



could be masked by the turbulent nature of the flame structure itself.

With a comparison of density ratios, it is necessary to note that experimental results<sup>(5)</sup> are given with extreme bounds on density ratios of 0.13 to 0.22. These were effected by varying the approach speed temperature from 294°K to 520°K with resultant increases in flame temperature from 2270°K to 2370°K.<sup>(8)</sup> The experimental results given in Figure 8, Reference 5, show a ratio of wake width at high density ratio to that at low density ratio of approximately 0.9, at a distance five duct heights downstream from the flameholder. Now, this change in initial temperature will also result in approximately a two-fold increase in laminar flame speed. The extremes of density ratios which have been calculated from this analysis are from 0.16 to 0.24. If we compare the results for a density ratio of 0.24 and  $\gamma$  of 0.2 with a density ratio of 0.16, we must select a  $\gamma$  of approximately 0.15 to take into account the change in laminar flame speed which would be engendered by change in approach temperature. From Figures 7 and 8 it is seen that the ratio of wake widths, at arbitrary downstream distances comparable to regions of experimental results, has a range of values from approximately 0.89 to 0.93.

This close agreement between experimental results and analytical results is not completely significant, since conditions were not completely the same, and there is an artificiality in selecting the results compared here. What is significant is that the theory does predict the right sense of change compared to experiments, and the relative magnitude is approximately correct, in contrast to earlier theories.

It has been observed experimentally that changing the fuel-air ratio has only a slight effect on the flame spreading rate, but that the

small effect observed is embodied by an increase in rate on either side of the stoichiometric mixture. If the fuel-air equivalence ratio is decreased, the effect is to increase the density ratio  $\lambda$ , at the same time decreasing the laminar flame velocity, thereby effecting a decrease in  $\gamma$ . This behavior would suggest a flame spreading rate that was greatest at the rich end of supportable combustion and that decreased with decreasing fuel-air ratio to the lean limit of combustion.

While the sense of this change agrees with experimental results from stoichiometric to the fuel-rich portion, the sense is opposite from experimental results in the fuel-lean region. This inconsistency with experimental results suggests that ignoring the chemical effects may lead to some difficulty. Despite this obvious shortcoming, the analysis shows promise of utility through its agreement with other conclusions that have been drawn from experimental results.

### III. CONCLUDING REMARKS

The parametric relations between gas velocities and wake width were reviewed, and comparisons made with experimental values. The agreement is good for the area beyond the local influence of the flameholder. A series representation for the cold gas velocity in terms of the density ratio and wake width was developed. Values have been computed utilizing the first four terms of the series for representative values of the density ratio. These values show excellent agreement out to a dimensionless wake width of 0.6; however, rapid divergence occurs beyond 0.7.

An attempt to develop the wake spreading rate in the axial direction was made using the momentum equation. Solution of the integral equation was possible using the series representation of the cold gas velocity, but led to a physically inadmissible result. The technique was varied by utilizing the moment of the momentum equation, also without success. A numerical solution utilizing the parametric relations developed failed in a similar manner, indicating a weakness in the basic approach rather than in the series representation.

A solution for the wake spreading rate was obtained, through a continuity equation into the flame front, after defining an effective turbulent flame velocity. This was defined to consist of the laminar flame velocity plus a component proportional to the local velocity gradient in the hot gas. The constant of proportionality was evaluated by comparison with experimental results. The wake spreading rate was found to vary little with a change in approach gas velocity. This appears qualitatively consistent with experimentally derived results. A decrease in the density

ratio predicts an increase in the wake spreading rate. A change of 50 per cent results in the same magnitude variation in theory and in experiments. It has been experimentally observed that the spreading rate is a minimum near a stoichiometric mixture. This is not found to be the case from this analysis, if the assumption is made that increasing the equivalence ratio results in only an increase in the flame temperature, and hence an increase in laminar flame speed and a decrease in density ratio. The prediction is for a monotonically-increasing flame spreading rate for an increasing equivalence ratio.

## REFERENCES

1. Scurlock, A. C., "Flame Stabilization and Propagation in High Velocity Gas Streams," Meteor. Report No. 19, Cambridge, Massachusetts Institute of Technology (May, 1948).
2. Tsien, H. S., "Influence of Flame Fronts on the Flow Field," Journal of Applied Mechanics, Vol. 18 (1951), pp. 188-194.
3. Spalding, D. B., "Ends and Means in Flame Theory," Sixth Symposium (International) on Combustion, Williams and Wilkins Co. (1956).
4. Wright, F. H. and Zukoski, E. E., "Flame Spreading from Bluff Body Flameholders," NASA Technical Release No. 34-17, Jet Propulsion Laboratory, Pasadena, California (May 11, 1960).
5. Satre, R. S., "An Experimental Investigation of Flame Propagation Downstream of a Cylindrical Flameholder," Ae. Thesis, California Institute of Technology, Pasadena (1959).
6. Thurston, D. W., "An Experimental Investigation of Flame Spreading from Bluff Body Flameholders," Ae. Thesis, California Institute of Technology, Pasadena (1958).
7. Utterback, P. W., "An Experimental Investigation of Flow Conditions Behind a Bluff Body Flameholder," Ae. Thesis, California Institute of Technology, Pasadena (1960).
8. Huntley, S. C., "Ideal Temperature Rise Due to Constant Pressure Combustion of a JP-4 Fuel," NACA RM E55G27a, Cleveland (September 27, 1955).

TABLE I. Gas Velocities at Various Wake Widths.

$c$	$\lambda = .16$		$\lambda = .20$		$\lambda = .24$	
	$\alpha$	$\beta$	$\alpha$	$\beta$	$\alpha$	$\beta$
0.02	1.01696	1.10053	1.01614	1.07763	1.01533	1.06201
0.04	1.03424	1.19469	1.03257	1.15175	1.03090	1.12201
0.06	1.05191	1.28433	1.04933	1.22327	1.04677	1.18048
0.08	1.06998	1.37101	1.06644	1.29302	1.06295	1.23789
0.10	1.08850	1.45561	1.08394	1.36154	1.07946	1.29457
0.13	1.11719	1.58017	1.11097	1.46291	1.10490	1.37878
0.16	1.14705	1.70342	1.13901	1.56358	1.13120	1.46265
0.20	1.18888	1.86792	1.17810	1.69814	1.16773	1.57493
0.24	1.23324	2.03470	1.21936	1.83453	1.20610	1.68873
0.30	1.30521	2.29331	1.28582	2.04545	1.26752	1.86432
0.40	1.44252	2.76060	1.41105	2.42347	1.38197	2.17687
0.50	1.60768	3.29635	1.55905	2.8505	1.51513	2.52547
0.60	1.81075	3.93330	1.73721	3.34823	1.67249	2.92494
0.70	2.06695	4.71778	1.95625	3.94588	1.86169	3.39440
0.80	2.40079	5.72233	2.23250	4.68660	2.09390	3.96071
0.90	2.85450	7.07030	2.59228	5.63881	2.38609	4.66400
1.00	3.50746	8.99254	3.08077	6.91923	2.76541	5.56792

TABLE II. Coefficients of Power Series for Cold Velocity

<u>c</u>	<u>f</u>	<u>g</u>	<u>h</u>
.2	-0.0685	-0.1328	-0.0080
.3	-0.143	-0.198	+0.0243
.4	-0.259	-0.250	+0.186
.5	-0.433	-0.250	+0.325
.6	-0.714	-0.0094	+0.558
.7	-1.200	+0.584	+0.428
.8	-2.200	+3.500	-4.621

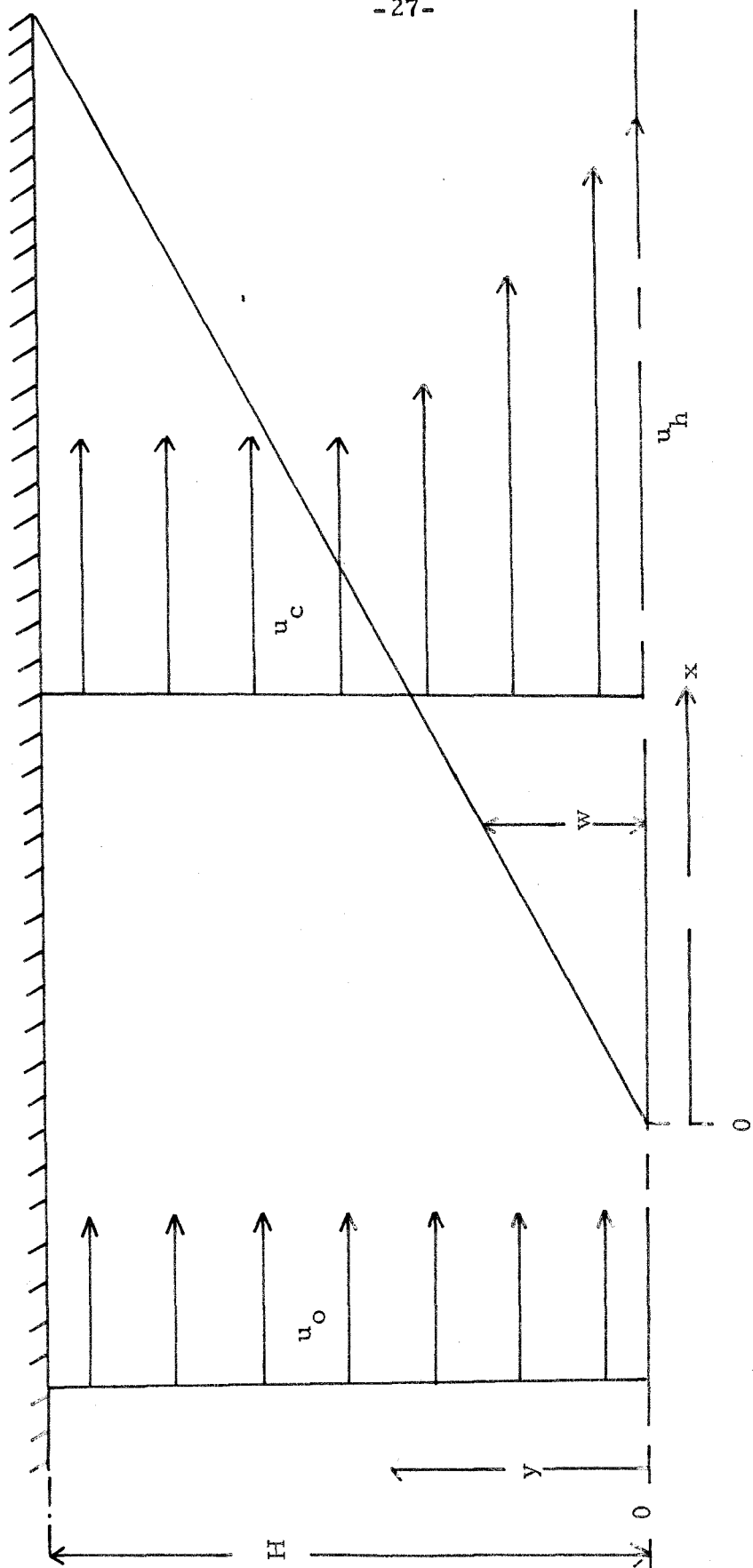


Figure 1. Model of Flow for Analysis.



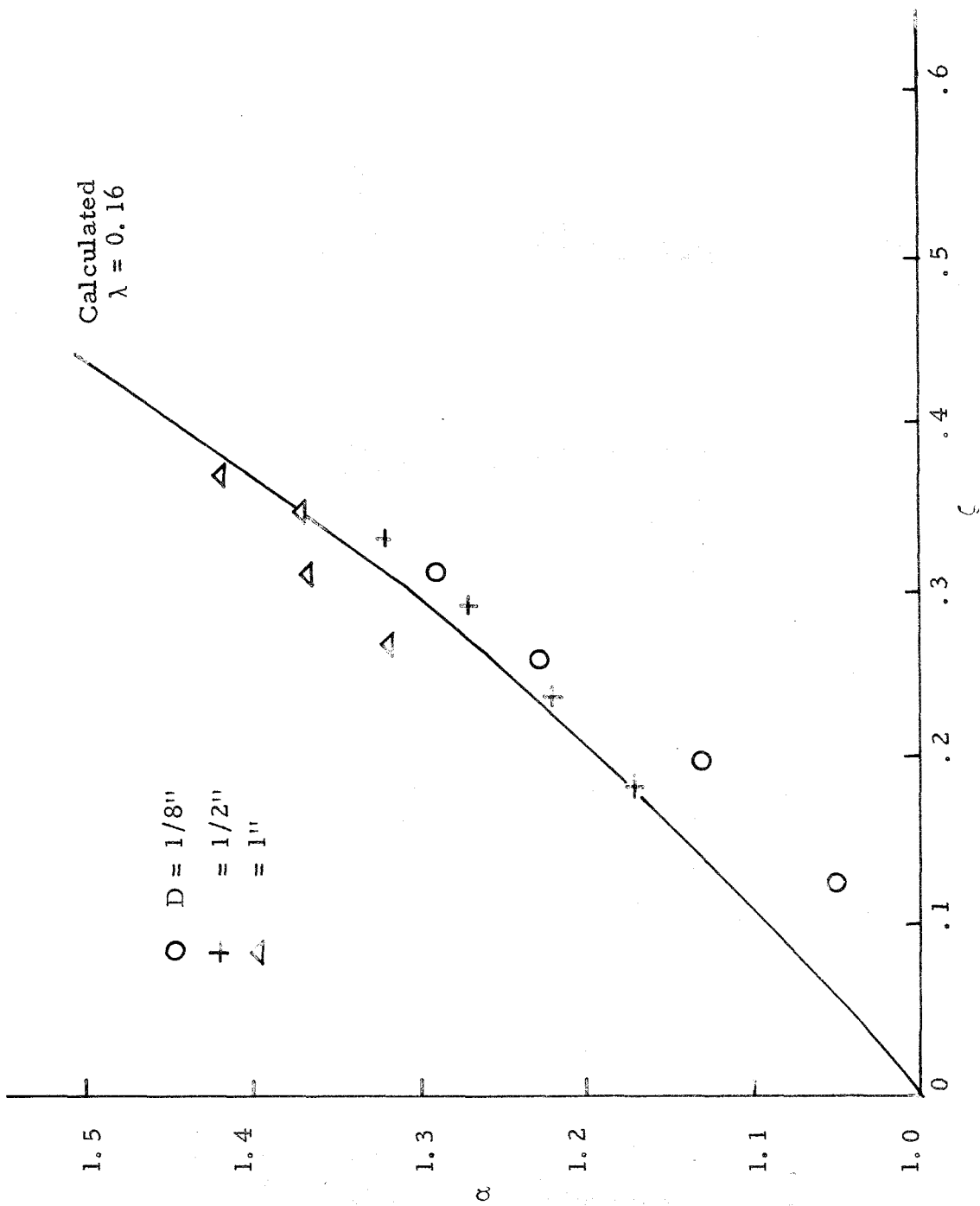


Figure 2. Gas Velocity Versus Wake Width.

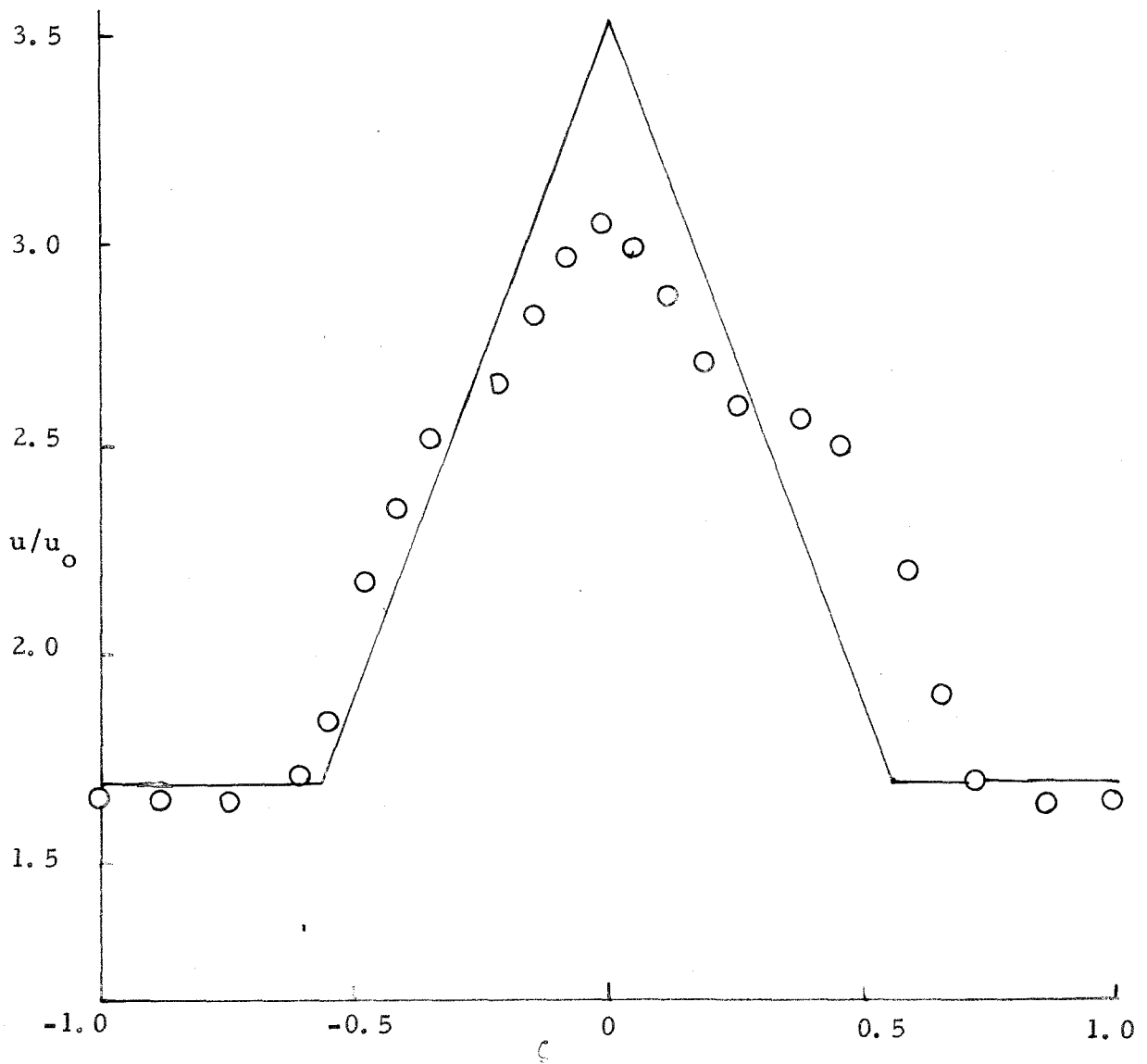


Figure 3. Comparison of Velocity Profiles.

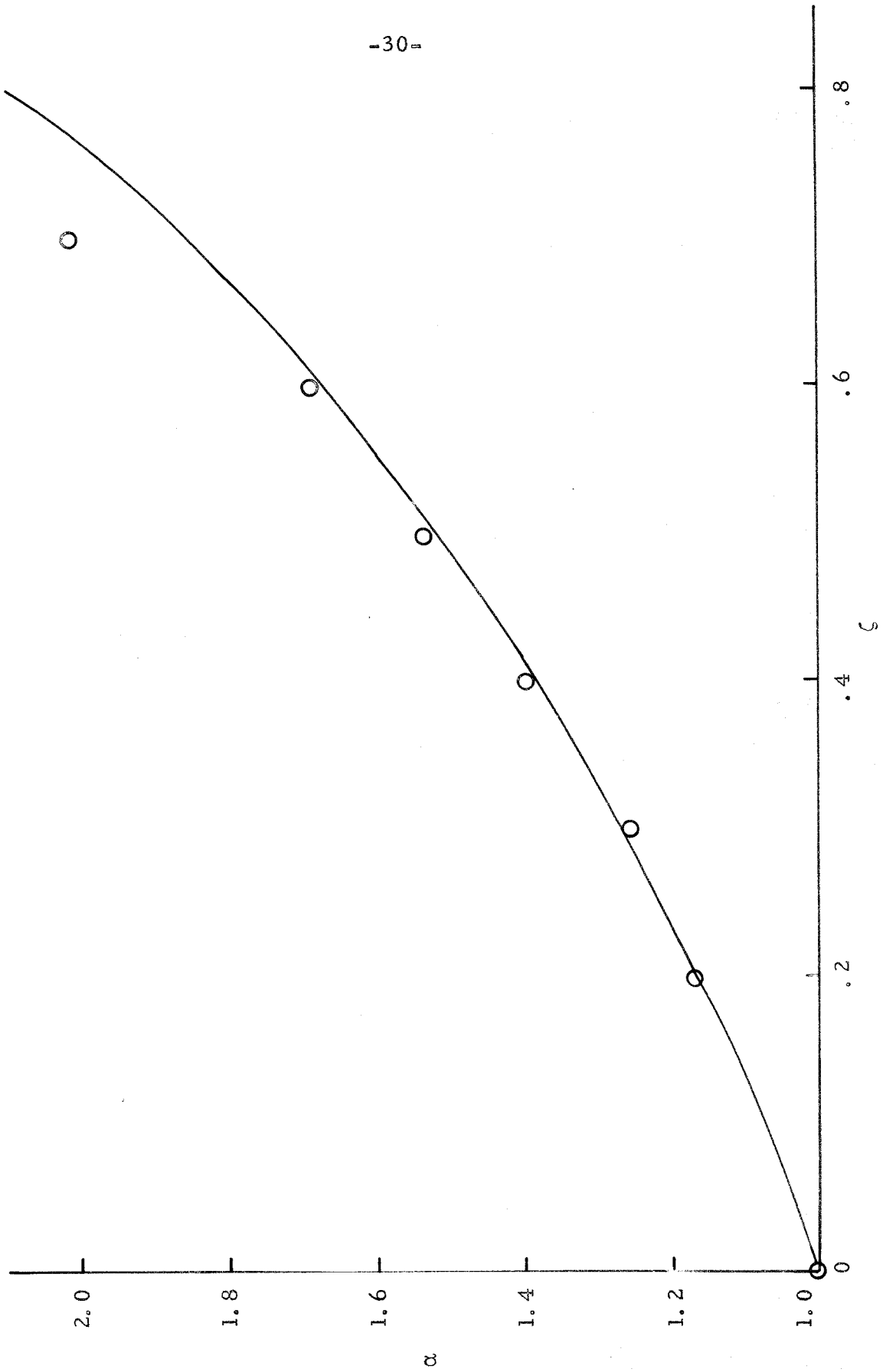


Figure 4. Comparison of Series for  $\lambda = 0.24$ .

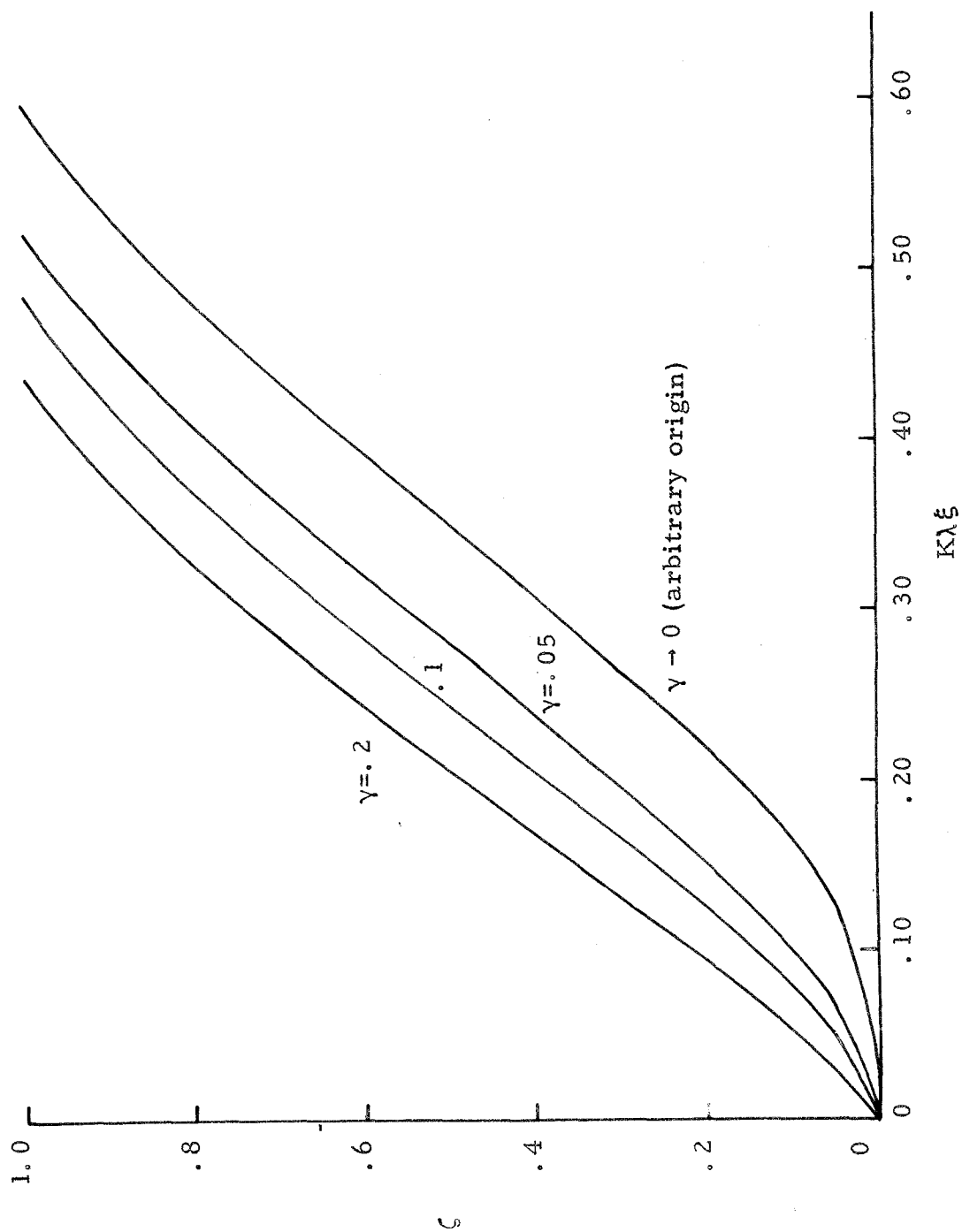


Figure 5. Wake Spreading for  $\lambda = .16$ .

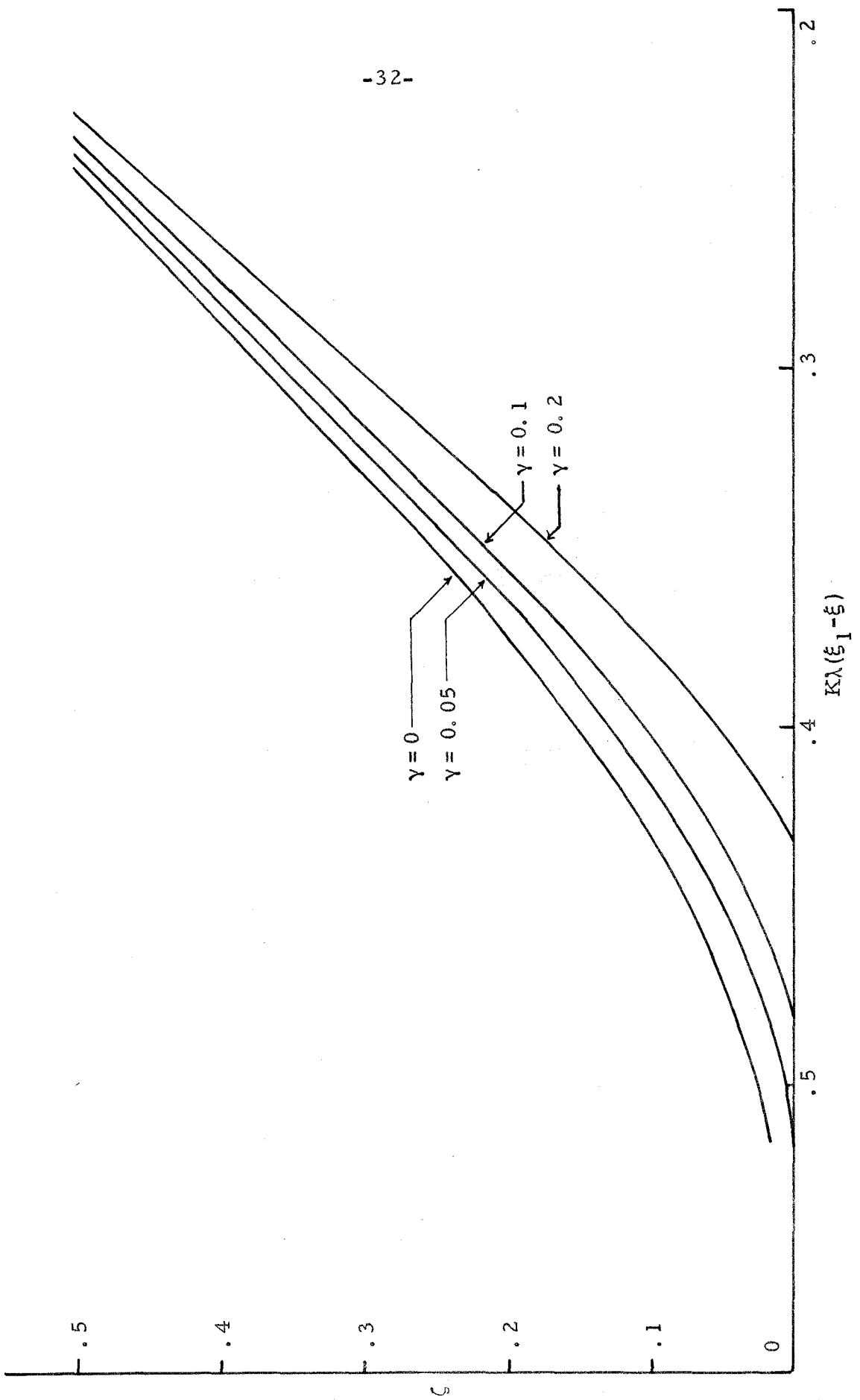


Figure 6. Wake Spreading for  $\lambda = .16$ .

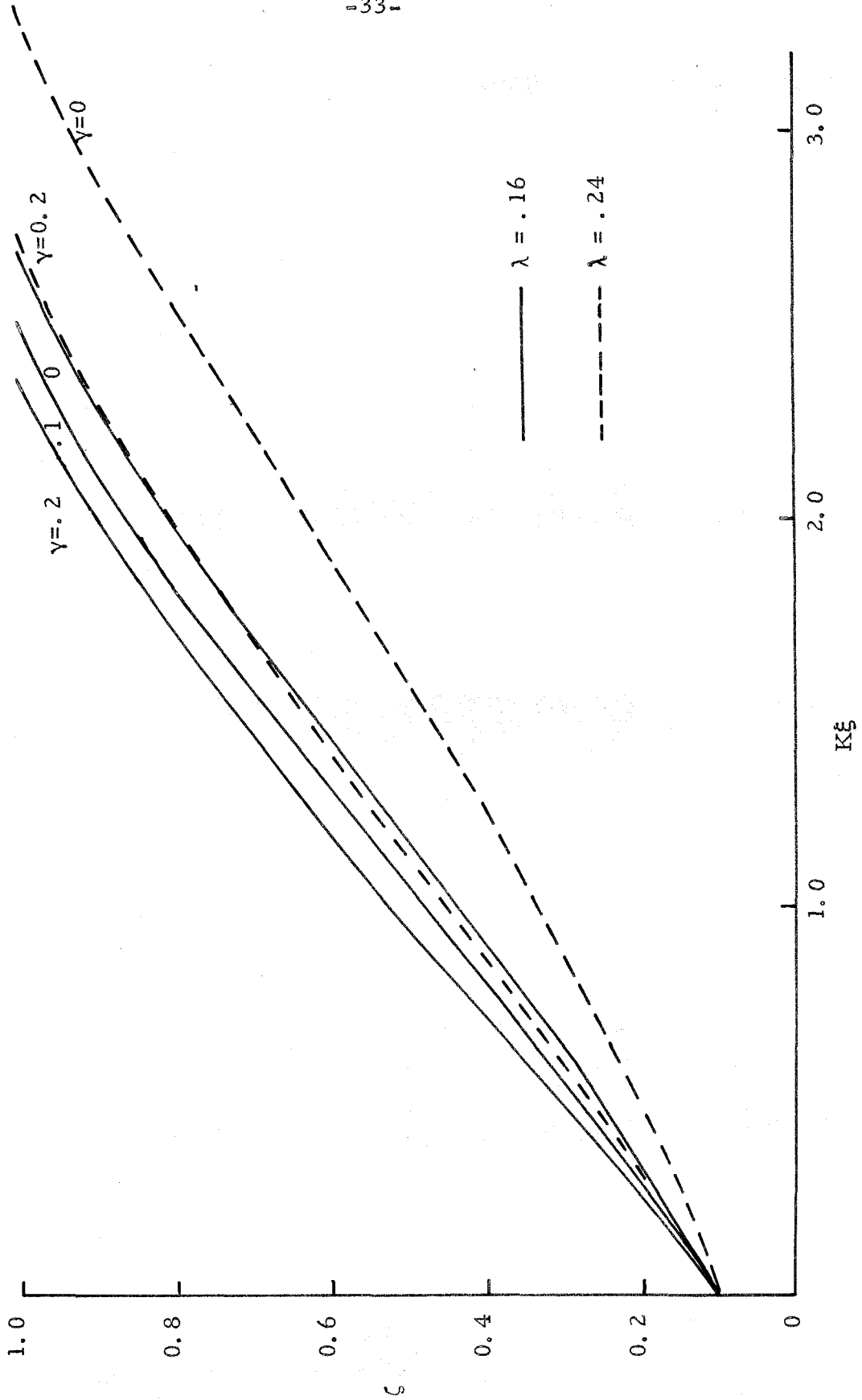


Figure 7. Spreading Rate with Initial Wake Width of 0.1 .

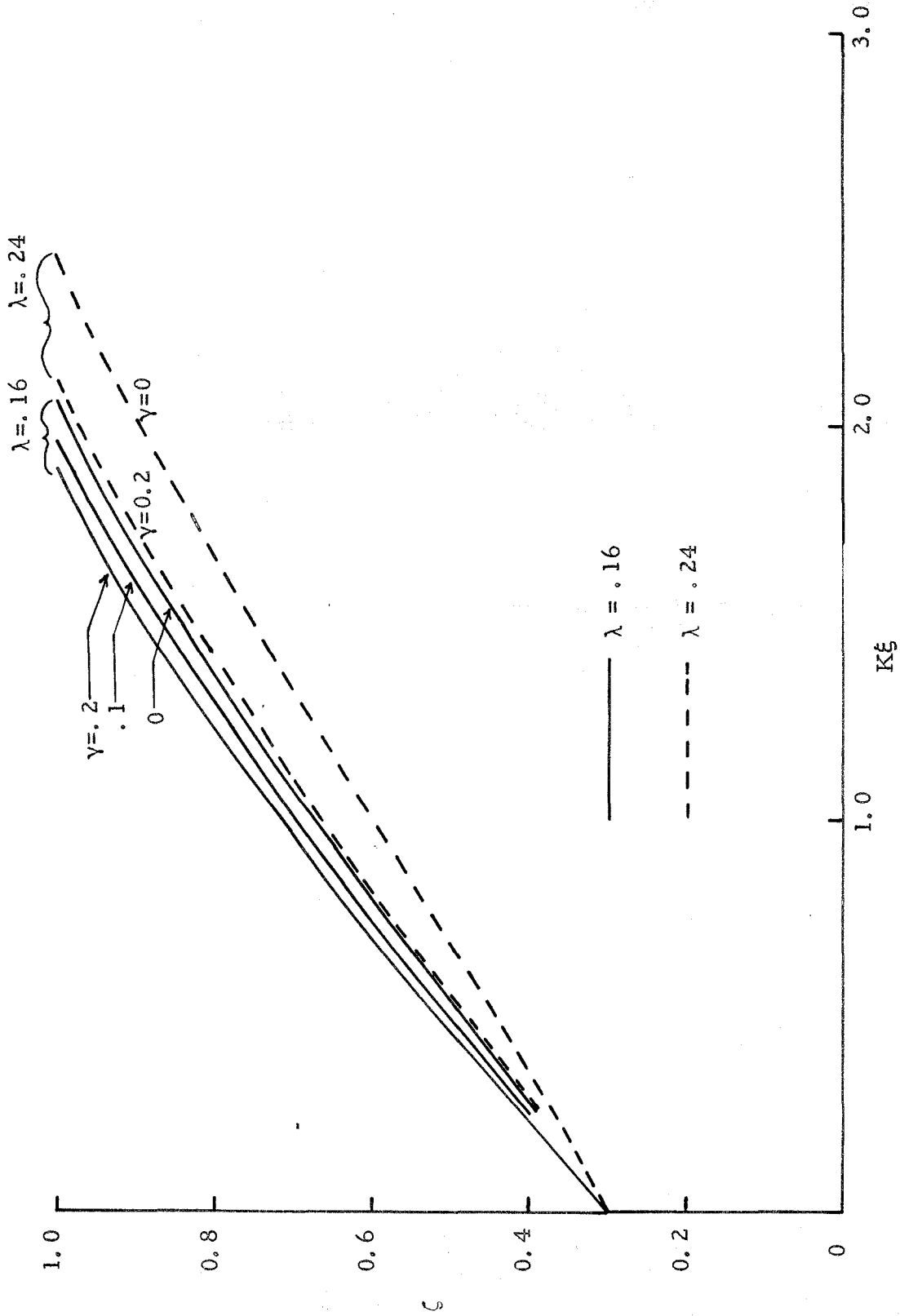


Figure 8. Spreading Rate with Initial Wake Width of 0.3 .